Supplementary Material

Table S1. Precipitation related natural proxies Ljungqvist et al. (2016)

NAME	Lat (°N)	Long (°E)	Archive type	season	Temporal resolution	Reference
Bunker Cave	7.66	51.37	Speleothem	winter	multi-centennial to multi-decadal	Fohlmeister et al. (2012)
Central Europe	9	50	Tree-ring width	summer	500-2000 AD	Büntgen and Tegel (2011)
Fagelmossen	114.27	59.29	OTH	annual	4500-700 cal yr BP	Borgmark and Wastegård (2008)
Fagelmossen	114.27	59.29	OTH	annual	4500-700 cal yr BP	Borgmark and Wastegård (2008)
Germany	9	51.5	Tree-ring	summer	1000-2000 AD	Büntgen et al. (2010)
Klapferloch Cave	10.55	47.95	Speleothem	annual	0-3000 yr a b2k	Boch and Spötl (2011)
Kontolanrahka	22.78	60.78	Lake sediment	annual	last 5000 cal yr BP	Väliranta et al. (2007)
Lake Allos	6.7	44.23	Lake sediment	annual	700 - 2000 AD	Wilhelm et al. (2012)
Lake Anterne	6.47	45.59	Lake sediment	annual	9950 - 5550 cal yr BP	Giguet-Covex et al. (2011)
Lake Hackren	13.5	63.17	peat bogs	annual	5000 BC - 2006 AD	Gunnarson (2008)
Lake Mondsee	13.4	47.81	Lake sediment	annual	400–2005 AD	Swierczynski et al. (2012)
Lake Shkodra	19.5	42.1	Lake sediment	annual	last 4500 cal a BP	Zanchetta et al. (2012)
Lake le Bourget	5.68	45.82	Lake sediment	annual	4500-3500 cal a BP	Magny et al. (2012)
Lille Vildmose	10.22	56.88	peat bogs	annual	2150 BC - 1830 AD	Mauquoy et al. (2008)
Nerfloen	26.25	58.87	peat bogs	annual	last 4200 cal yr BP	Vasskog et al. (2012)
Mannikjarve Bog	19.7	47.99	Lake sediment	annual	last 45000 cal yr BP	Sillasoo et al. (2007)
NadasLake	6.87	61.93	Lake sediment	winter	last 2000 AD yrs	Sümegi et al. (2009)
Stomyren	113.27	60.21	peat bogs	annual	4500-700 cal yr BP	Borgmark and Wastegård (2008)
Store Mosse Bog	14.12	57.25	peat bogs	annual	1500 cal yr BP- 1900 AD	Jong et al. (2007)
Swiss Alps	8	46.3	Tree-ring	summer	900 - 1350 AD	Kress et al. (2014)

• a b2k (before the year AD 2000), cal yr BP (calibrated years before the present)

Table S2. Temperature related natural proxies Ljungqvist et al. (2016)

NAME	Lat (°N)	Long (°E)	Archive type	season	Temporal resolution	Reference
Albania	20	41	Tree ring	summer	968 - 2008 AD	Seim et al. (2012)
The Alps	8	46.3	Tree ring	summer	755 - 2005 AD	Büntgen et al. (2006)
CentralEurope	8	46	Tree ring	summer	962 - 2007 AD	Büntgen et al. (2011)
Central England	2	52	Written evidence	annual	900 -1950 AD	Lamb (1965)
DeBilt summer	5.18	52.1	Written evidence	summer	800 - 2000 AD	Van Engelen et al. (2001)
DeBilt winter	5.18	52.1	Written evidence	winter	800 - 2000 AD	Van Engelen et al. (2001)
Eastern Carpathians	25.1	47.2	Tree ring	summer	1163 - 2005 AD	Popa and Kern (2009)
Gulf of Taranto	17.88	39.75	SEA	annual	200 BC - 2000 AD	Taricco et al. (2009)
Jamtland	13.3	63.1	Tree ring	summer	450BC - 1900 AD	Linderholm and Gunnarson (2005)
Lake Korttajarvi	25	62	Lake sediment	annual	8000 BC - 2000 AD	Tiljander et al. (2006)
Lake Lehmilampi	29	63	Lake sediment	annual	last 2000 yrs	Haltia-Hovi et al. (2007)
Lake Nautajarvi	24	61	Lake sediment	annual	8000 BC - 2000 AD	Ojala and Alenius (2005)
MD95 2011	7.64	66.97	SEA	summer	last 13000 yr B.P	Berner et al. (2011)
NorthernSpain	-3.5	42.9	Speleothem	annual	last 4000 yr BP	Martín-Chivelet et al. (2011)
Norwegian Sea	5.26	63.76	SEA	annual	2000 BC- 1000 AD	Sejrup et al. (2010)
Spannagel Cave	11.4	47.05	Speleothem	annual	2000 BP yrs - 1 AD	Mangini et al. (2005)
Vallee des Merveilles	7.28	44.05	Tree ring	summer	1356 - 2007 AD	Büntgen and Tegel (2011)

MAE calibration

	GR1A_Model(Gridded)	BRNN(Gridded)	LSTM(Gridded)	BRNN(Gridded+Proxies)	LSTM(Gridded+Proxies)	BRNN(Gridded+PDSI)	LSTM(Gridded+PDSI)	BRNN(Gridded+Lag)	LSTM(Gridded+Lag)
Orsova-Danube	37	24	22	20	16	22	19	19	14
Decin-Elbe	41	27	24	26	21	25	22	23	21
Dresden-Elbe	39	27	26	27	22	26	28	24	23
Elverum-Glama	55	46	38	43	41	44	43	45	36
Vargoens KRV- Goeta	98	58	48	59	60	57	53	42	40
Wasserburg-Inn	99	54	50	53	40	53	53	52	37
Muroleekoski-Kokemenjoki	72	36	23	36	36	34	35	31	33
Blois-Loire	42	39	34	37	32	40	29	35	31
Montjean-Loire	40	33	29	33	26	34	26	29	25
NeuerHafen-Main	42	38	35	37	33	36	35	35	33
Wuerzburg-Main	46	42	38	41	40	40	36	38	28
Smalininkai-Nemunas	62	24	24	24	23	23	22	22	20
BaselRheinhalle-Rhine	108	64	60	55	52	59	57	61	46
Baselschifflaende-Rhine	107	61	54	52	50	57	61	57	46
Koeln-Rhine	44	38	35	35	35	37	33	32	24
Rees-Rhine	46	37	32	35	26	35	33	32	27
Burghausen-Salzach	106	105	87	100	84	87	64	106	80
Hann-Munden-Wesser	37	34	32	33	32	34	32	30	24
Bodenwerder-Wesser	38	33	30	33	33	33	32	30	21
Vlotho-Wesser	44	34	33	34	46	34	32	30	32
Intschede-Wesser	40	34	30	33	28	34	34	29	31

MAE validation

	GR1A_Model(Gridded)	BRNN(Gridded)	LSTM(Gridded)	BRNN(Gridded+Proxies)	LSTM(Gridded+Proxies)	BRNN(Gridded+PDSI)	LSTM(Gridded+PDSI)	BRNN(Gridded+Lag)	LSTM(Gridded+Lag)
Orsova-Danube	78	28	28	40	33	26	25	28	30
Decin-Elbe	62	29	30	31	33	28	28	28	27
Dresden-Elbe	50	31	32	33	34	32	31	29	29
Elverum-Glama	72	66	64	105	68	69	63	64	79
Vargoens KRV- Goeta	64	55	71	57	55	52	56	54	50
Wasserburg-Inn	125	61	63	60	68	62	62	60	65
Muroleekoski-Kokemenjoki	79	46	28	46	47	43	45	43	43
Blois-Loire	44	34	32	41	43	33	33	35	36
Montjean-Loire	44	37	40	37	37	36	38	31	33
NeuerHafen-Main	51	40	42	44	42	40	42	35	33
Wuerzburg-Main	59	34	39	35	43	31	36	32	36
Smalininkai-Nemunas	44	26	26	28	28	25	26	28	27
BaselRheinhalle-Rhine	98	72	73	74	82	69	67	69	75
Baselschifflaende-Rhine	96	73	73	82	77	70	64	70	69
Koeln-Rhine	48	33	32	62	55	35	34	32	33
Rees-Rhine	51	35	37	45	50	38	39	35	37
Burghausen-Salzach	44	146	154	142	149	162	167	144	164
Hann-Munden-Wesser	56	33	33	45	46	34	35	30	35
Bodenwerder-Wesser	46	38	36	43	40	38	36	35	45
Vlotho-Wesser	70	56	51	72	47	57	52	54	50
Intschede-Wesser	48	44	42	40	42	43	40	41	38

RMSE calibration

	GR1A_Model(Gridded)	BRNN(Gridded)	LSTM(Gridded)	BRNN(Gridded+Proxies)	LSTM(Gridded+Proxies)	BRNN(Gridded+PDSI)	LSTM(Gridded+PDSI)	BRNN(Gridded+Lag)	LSTM(Gridded+Lag)
Orsova-Danube	47	29	28	24	23	27	25	24	20
Decin-Elbe	52	34	33	33	30	32	30	29	28
Dresden-Elbe	49	34	34	34	31	33	37	32	31
Elverum-Glama	71	58	52	55	57	55	55	57	49
Vargoens KRV- Goeta	116	71	65	69	75	69	67	51	51
Wasserburg-Inn	126	71	68	69	57	70	72	69	54
Muroleekoski-Kokemenjoki	87	47	33	47	47	44	45	40	42
Blois-Loire	54	50	46	47	44	50	41	44	43
Montjean-Loire	50	43	39	42	48	43	37	35	35
NeuerHafen-Main	52	50	48	48	46	47	46	45	43
Wuerzburg-Main	58	54	50	51	55	51	46	48	39
Smalininkai-Nemunas	70	33	33	33	33	32	32	31	29
BaselRheinhalle-Rhine	130	79	77	71	71	75	75	77	64
Baselschifflaende-Rhine	128	74	70	66	68	71	78	71	60
Koeln-Rhine	52	48	47	43	51	47	44	40	34
Rees-Rhine	59	47	43	42	40	45	43	40	35
Burghausen-Salzach	139	131	123	128	118	114	97	131	111
Hann-Munden-Wesser	46	45	44	43	42	44	43	38	33
Bodenwerder-Wesser	46	45	42	44	45	45	44	38	28
Vlotho-Wesser	53	45	45	44	59	45	44	37	41
Intschede-Wesser	49	45	42	43	40	45	45	37	40

RMSE validation

	GR1A_Model(Gridded)	BRNN(Gridded)	LSTM(Gridded)	BRNN(Gridded+Proxies)	LSTM(Gridded+Proxies)	BRNN(Gridded+PDSI)	LSTM(Gridded+PDSI)	BRNN(Gridded+Lag)	LSTM(Gridded+Lag)
Orsova-Danube	91	35	35	51	42	32	32	36	39
Decin-Elbe	75	37	38	39	43	37	36	36	35
Dresden-Elbe	62	40	41	41	44	41	40	37	38
Elverum-Glama	94	90	88	144	92	95	85	90	107
Vargoens KRV- Goeta	81	66	84	69	66	67	69	65	59
Wasserburg-Inn	146	74	76	74	83	74	77	74	79
Muroleekoski-Kokemenjoki	98	61	35	61	64	60	61	56	57
Blois-Loire	53	42	43	54	55	42	44	45	47
Montjean-Loire	53	45	49	48	46	44	47	42	44
NeuerHafen-Main	68	49	51	54	51	50	53	45	43
Wuerzburg-Main	70	42	49	44	52	37	45	39	45
Smalininkai-Nemunas	52	33	33	35	35	32	33	34	33
BaselRheinhalle-Rhine	117	88	90	88	100	84	83	81	87
Baselschifflaende-Rhine	115	89	89	95	92	85	76	82	84
Koeln-Rhine	59	42	43	74	69	45	44	41	44
Rees-Rhine	64	54	54	63	65	56	59	54	56
Burghausen-Salzach	52	181	182	173	188	202	208	178	195
Hann-Munden-Wesser	67	42	43	58	58	43	46	38	44
Bodenwerder-Wesser	57	47	45	53	53	47	47	43	54
Vlotho-Wesser	84	68	63	88	63	70	64	65	63
Intschede-Wesser	56	56	52	50	51	55	50	51	48

Table S3. Same as Tab. 3 but for MAE and RMSE

D calibration

Station	GR1A_Model(Gridded)	BRNN(Gridded)	LSTM(Gridded)	BRNN(Gridded+Proxies)	LSTM(Gridded+Proxies)	BRNN(Gridded+PDSI)	LSTM(Gridded+PDSI)	BRNN(Gridded+Lag)	LSTM(Gridded+Lag)
Orsova-Danube	0.84	0.91	0.92	0.94	0.95	0.92	0.94	0.94	0.96
Decin-Elbe	0.78	0.88	0.9	0.89	0.91	0.9	0.92	0.92	0.92
Dresden-Elbe	0.8	0.88	0.9	0.88	0.9	0.89	0.85	0.9	0.91
Elverum-Glama	0.78	0.82	0.88	0.85	0.81	0.84	0.85	0.83	0.89
Vargoens KRV- Goeta	0.59	0.54	0.71	0.56	0.26	0.59	0.65	0.85	0.84
Wasserburg-Inn	0.77	0.86	0.87	0.86	0.92	0.86	0.86	0.87	0.93
Muroleekoski-Kokemenjoki	0.68	0.87	0.7	0.87	0.89	0.9	0.89	0.92	0.91
Blois-Loire	0.9	0.91	0.93	0.92	0.92	0.91	0.94	0.93	0.94
Montjean-Loire	0.89	0.92	0.94	0.92	0.89	0.92	0.95	0.95	0.95
NeuerHafen-Main	0.83	0.81	0.84	0.83	0.84	0.84	0.85	0.86	0.88
Wuerzburg-Main	0.81	0.78	0.83	0.8	0.74	0.81	0.84	0.84	0.9
Smalininkai-Nemunas	0.5	0.61	0.57	0.62	0.65	0.66	0.69	0.7	0.75
BaselRheinhalle-Rhine	0.83	0.92	0.93	0.93	0.94	0.93	0.92	0.92	0.95
Baselschifflaende-Rhine	0.84	0.93	0.94	0.94	0.94	0.93	0.91	0.93	0.96
Koeln-Rhine	0.92	0.92	0.93	0.94	0.91	0.92	0.94	0.95	0.96
Rees-Rhine	0.9	0.92	0.94	0.94	0.95	0.93	0.93	0.94	0.96
Burghausen-Salzach	0.79	0.75	0.81	0.76	0.81	0.84	0.9	0.75	0.85
Hann-Munden-Wesser	0.9	0.88	0.9	0.89	0.91	0.88	0.9	0.92	0.94
Bodenwerder-Wesser	0.9	0.89	0.9	0.89	0.88	0.89	0.9	0.92	0.96
Vlotho-Wesser	0.86	0.89	0.9	0.89	0.8	0.89	0.91	0.93	0.92
Intschede-Wesser	0.86	0.86	0.9	0.87	0.91	0.86	0.87	0.92	0.91

D validation

Station	GR1A_Model(Gridded)	BRNN(Gridded)	LSTM(Gridded)	BRNN(Gridded+Proxies)	LSTM(Gridded+Proxies)	BRNN(Gridded+PDSI)	LSTM(Gridded+PDSI)	BRNN(Gridded+Lag)	LSTM(Gridded+Lag)
Orsova-Danube	0.58	0.84	0.83	0.71	0.65	0.85	0.85	0.85	0.84
Decin-Elbe	0.61	0.76	0.74	0.73	0.69	0.78	0.79	0.82	0.83
Dresden-Elbe	0.68	0.78	0.8	0.78	0.65	0.78	0.81	0.83	0.83
Elverum-Glama	0.54	0.56	0.66	0.47	0.58	0.54	0.59	0.55	0.59
Vargoens KRV- Goeta	0.59	0.49	0.56	0.47	0.33	0.55	0.55	0.61	0.61
Wasserburg-Inn	0.67	0.81	0.79	0.81	0.77	0.8	0.78	0.82	0.79
Muroleekoski-Kokemenjoki	0.56	0.66	0.55	0.66	0.7	0.66	0.68	0.71	0.71
Blois-Loire	0.85	0.89	0.89	0.82	0.78	0.89	0.89	0.89	0.86
Montjean-Loire	0.81	0.83	0.8	0.83	0.8	0.84	0.84	0.87	0.85
NeuerHafen-Main	0.71	0.73	0.72	0.67	0.73	0.75	0.72	0.81	0.84
Wuerzburg-Main	0.67	0.77	0.72	0.72	0.63	0.84	0.75	0.83	0.81
Smalininkai-Nemunas	0.59	0.5	0.44	0.51	0.47	0.56	0.57	0.58	0.6
BaselRheinhalle-Rhine	0.81	0.85	0.84	0.86	0.75	0.87	0.86	0.87	0.85
Baselschifflaende-Rhine	0.81	0.85	0.84	0.84	0.83	0.86	0.88	0.87	0.87
Koeln-Rhine	0.86	0.9	0.9	0.76	0.55	0.9	0.9	0.91	0.9
Rees-Rhine	0.86	0.86	0.87	0.82	0.77	0.86	0.82	0.87	0.87
Burghausen-Salzach	0.59	0.63	0.68	0.64	0.66	0.6	0.6	0.63	0.67
Hann-Munden-Wesser	0.7	0.8	0.8	0.68	0.73	0.8	0.78	0.86	0.82
Bodenwerder-Wesser	0.77	0.8	0.82	0.76	0.7	0.8	0.78	0.85	0.78
Vlotho-Wesser	0.62	0.7	0.73	0.61	0.73	0.7	0.74	0.76	0.79
Intschede-Wesser	0.79	0.76	0.79	0.8	0.81	0.76	0.8	0.82	0.85

KGE calibration

Station	GR1A_Model(Gridded)	BRNN(Gridded)	LSTM(Gridded)	BRNN(Gridded+Proxies)	LSTM(Gridded+Proxies)	BRNN(Gridded+PDSI)	LSTM(Gridded+PDSI)	BRNN(Gridded+Lag)	LSTM(Gridded+Lag)
Orsova-Danube	0.61	0.77	0.79	0.82	0.85	0.8	0.86	0.84	0.92
Decin-Elbe	0.61	0.71	0.76	0.73	0.71	0.75	0.83	0.79	0.79
Dresden-Elbe	0.65	0.72	0.78	0.72	0.76	0.74	0.66	0.76	0.77
Elverum-Glama	0.6	0.59	0.75	0.63	0.54	0.63	0.64	0.61	0.74
Vargoens KRV- Goeta	0.2	0.2	0.44	0.23	-0.02	0.25	0.33	0.65	0.59
Wasserburg-Inn	0.39	0.67	0.69	0.67	0.79	0.67	0.68	0.68	0.83
Muroleekoski-Kokemenjoki	0.46	0.7	0.41	0.7	0.75	0.74	0.75	0.79	0.78
Blois-Loire	0.81	0.77	0.83	0.78	0.72	0.76	0.87	0.82	0.85
Montjean-Loire	0.76	0.8	0.84	0.79	0.71	0.79	0.9	0.86	0.86
NeuerHafen-Main	0.68	0.58	0.64	0.6	0.61	0.62	0.67	0.67	0.71
Wuerzburg-Main	0.65	0.52	0.65	0.56	0.44	0.57	0.62	0.63	0.74
Smalininkai-Nemunas	-0.15	0.28	0.22	0.3	0.35	0.35	0.4	0.41	0.47
BaselRheinhalle-Rhine	0.66	0.79	0.85	0.82	0.86	0.81	0.8	0.8	0.83
Baselschifflaende-Rhine	0.66	0.81	0.88	0.84	0.84	0.83	0.76	0.82	0.92
Koeln-Rhine	0.84	0.8	0.82	0.82	0.79	0.81	0.87	0.86	0.85
Rees-Rhine	0.8	0.8	0.87	0.82	0.84	0.81	0.76	0.85	0.89
Burghausen-Salzach	0.61	0.48	0.61	0.49	0.58	0.63	0.72	0.47	0.66
Hann-Munden-Wesser	0.81	0.71	0.76	0.72	0.78	0.71	0.77	0.79	0.8
Bodenwerder-Wesser	0.81	0.72	0.75	0.72	0.68	0.72	0.76	0.8	0.87
Vlotho-Wesser	0.75	0.72	0.76	0.71	0.59	0.72	0.78	0.81	0.81
Intschede-Wesser	0.74	0.67	0.75	0.68	0.8	0.67	0.69	0.78	0.81

KGE validation

Station	GR1A_Model(Gridded)	BRNN(Gridded)	LSTM(Gridded)	BRNN(Gridded+Proxies)	LSTM(Gridded+Proxies)	BRNN(Gridded+PDSI)	LSTM(Gridded+PDSI)	BRNN(Gridded+Lag)	LSTM(Gridded+Lag)
Orsova-Danube	0.55	0.65	0.63	0.55	0.34	0.67	0.64	0.73	0.73
Decin-Elbe	0.49	0.51	0.49	0.46	0.43	0.58	0.57	0.65	0.67
Dresden-Elbe	0.49	0.56	0.61	0.57	0.34	0.59	0.64	0.63	0.66
Elverum-Glama	0.2	0.24	0.46	0.06	0.34	0.19	0.31	0.24	0.37
Vargoens KRV- Goeta	0.27	0.09	0.38	0.07	-0.36	0.18	0.16	0.39	0.34
Wasserburg-Inn	0.67	0.55	0.53	0.55	0.54	0.54	0.51	0.59	0.58
Muroleekoski-Kokemenjoki	0.28	0.38	0.25	0.38	0.48	0.37	0.41	0.44	0.44
Blois-Loire	0.73	0.75	0.74	0.66	0.53	0.75	0.77	0.79	0.72
Montjean-Loire	0.67	0.67	0.63	0.69	0.62	0.7	0.71	0.76	0.72
NeuerHafen-Main	0.47	0.42	0.41	0.38	0.42	0.47	0.43	0.53	0.59
Wuerzburg-Main	0.55	0.47	0.49	0.42	0.3	0.59	0.49	0.6	0.63
Smalininkai-Nemunas	0.28	0.16	0.08	0.17	0.1	0.23	0.26	0.31	0.32
BaselRheinhalle-Rhine	0.72	0.67	0.64	0.71	0.47	0.7	0.67	0.69	0.66
Baselschifflaende-Rhine	0.72	0.67	0.64	0.69	0.61	0.7	0.67	0.69	0.73
Koeln-Rhine	0.79	0.76	0.77	0.75	0.22	0.82	0.82	0.84	0.81
Rees-Rhine	0.77	0.62	0.68	0.64	0.5	0.66	0.55	0.7	0.71
Burghausen-Salzach	0.28	0.39	0.5	0.39	0.42	0.37	0.33	0.39	0.53
Hann-Munden-Wesser	0.54	0.53	0.53	0.45	0.54	0.55	0.53	0.66	0.65
Bodenwerder-Wesser	0.59	0.56	0.6	0.55	0.41	0.56	0.52	0.67	0.68
Vlotho-Wesser	0.38	0.48	0.49	0.41	0.44	0.49	0.54	0.61	0.68
Intschede-Wesser	0.59	0.52	0.57	0.56	0.6	0.53	0.56	0.67	0.76

Table S4. Same as Tab. 3 but for D and KGE

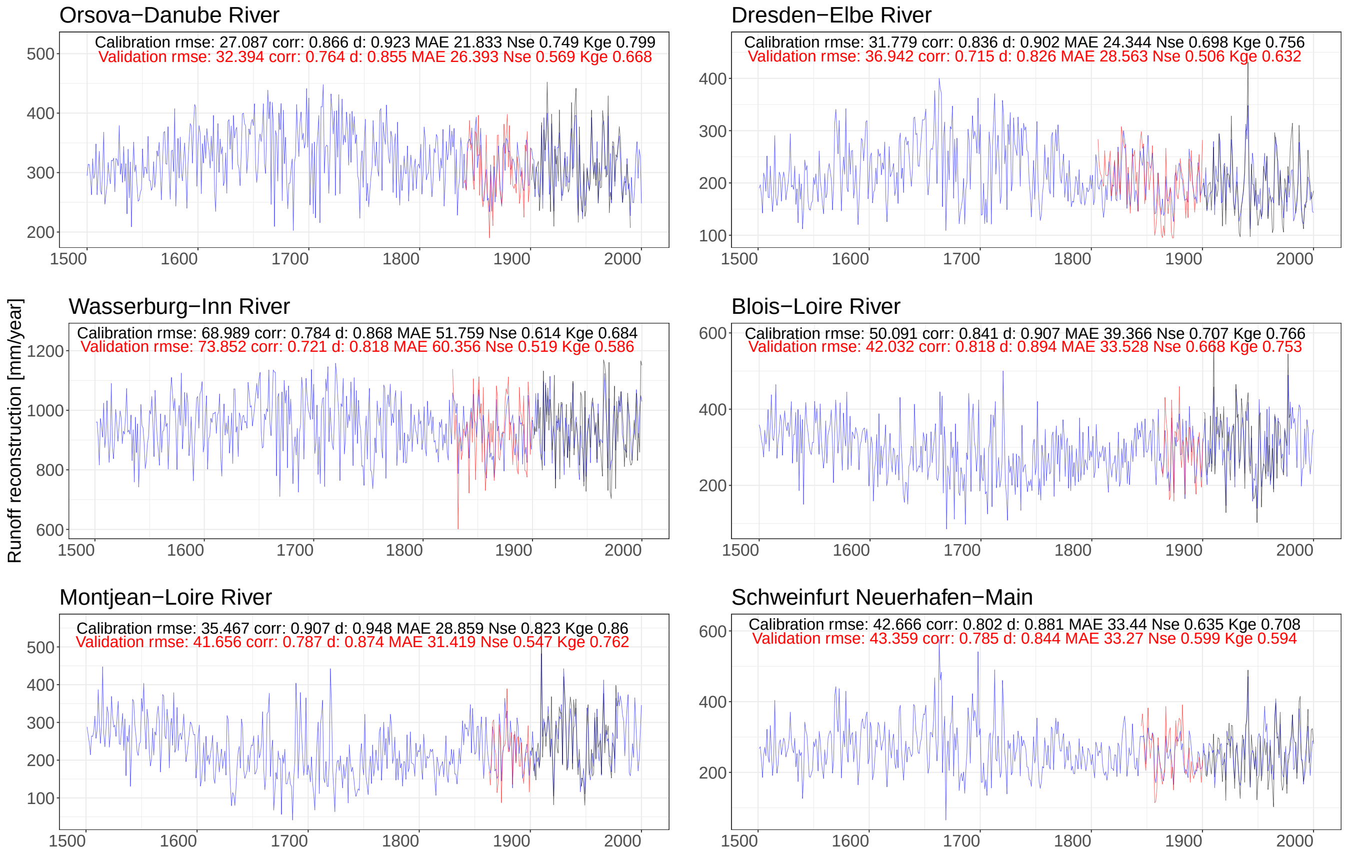

Figure S1. Reconstruction of Runoff over the past 500 years (data series are available in Orsova-Danube River, Dresden-Elbe River, Wasserburg-Inn River, Blois-Loire River, Montjean-Loire River, Schweinfurt Neuerhafen-Main. The black and red color indicate the GRDC observation runoff variable for calibrated and validated portion, whereas, the blue color represents reconstruction value of runoff simulated with the specific combinations. The observed statistic properties for calibration and validation data are displayed in top of the figure

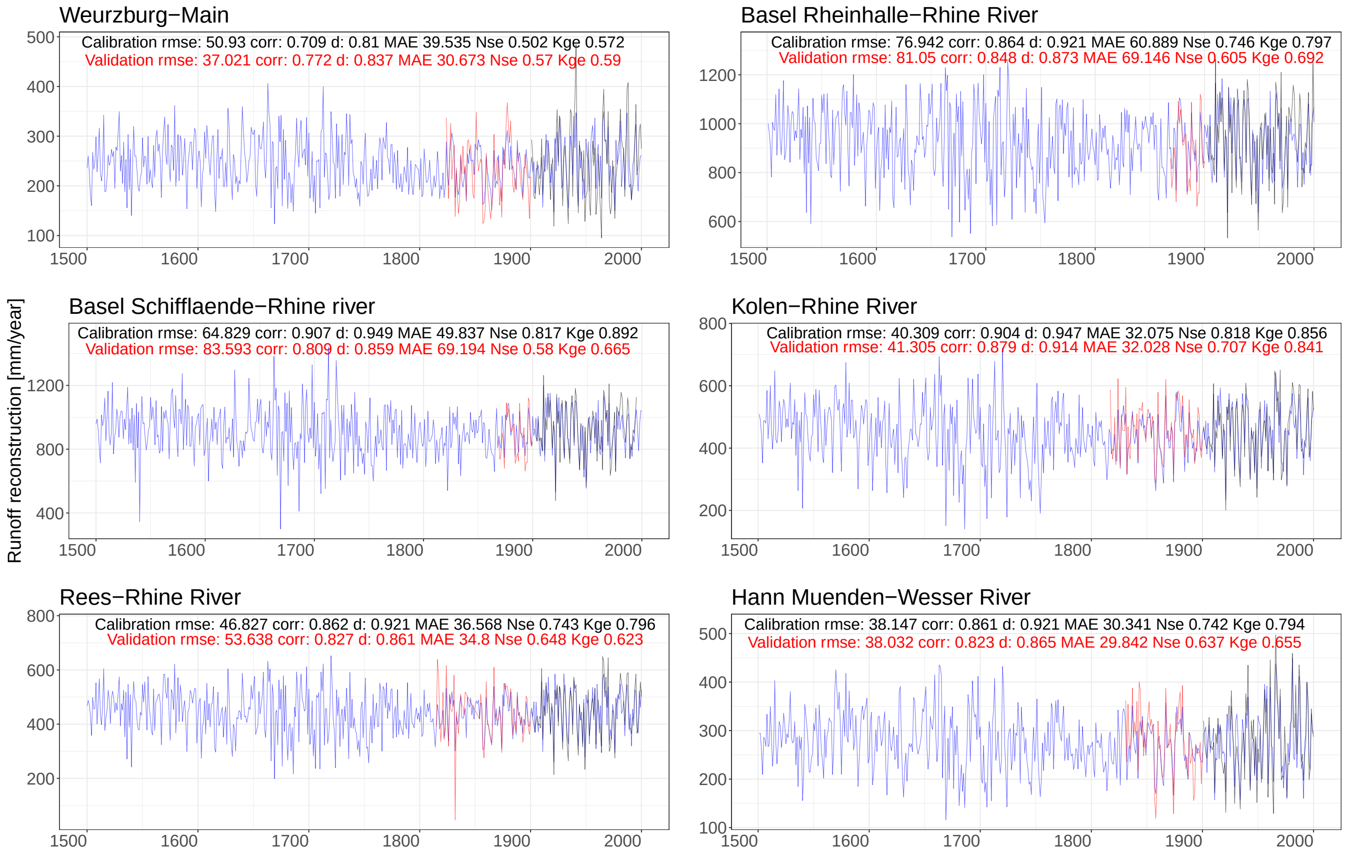

Figure S2. Same as Fig. S1 but runoff series are available in Weurzburg-Main, Basel Rheinhalle-Rhine River, Basel Schifflaende-Rhine river, Kolen-Rhine River, Rees-Rhine River, Hann Muenden-Wesser River.

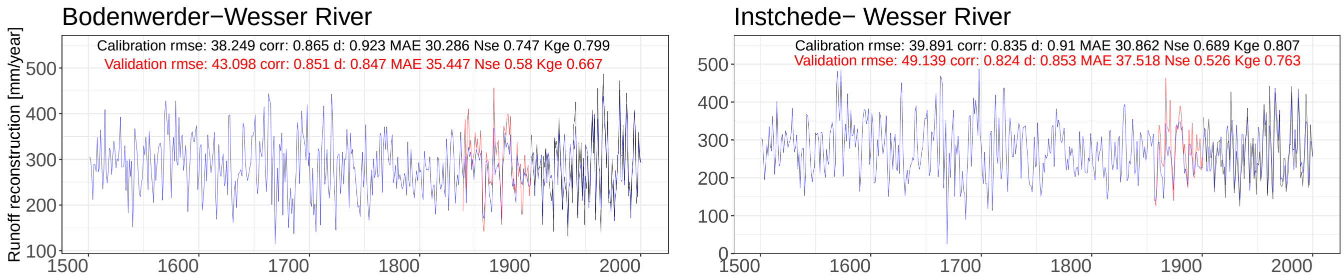

Figure S3. Same as Figs. S1 and S2 but for runoff series in Bodenwerder and Intschede - Wesser river

References

Berner, K., Koç, N., Godtliebsen, F., and Divine, D.: Holocene climate variability of the Norwegian Atlantic Current during high and low solar insolation forcing, Paleoceanography, 26, 2011.

Boch, R. and Spötl, C.: Reconstructing palaeoprecipitation from an active cave flowstone, Journal of Quaternary Science, 26, 675–687, 2011.

Borgmark, A. and Wastegård, S.: Regional and local patterns of peat humification in three raised peat bogs in Värmland, south-central Sweden, Gff, 130, 161–176, 2008.

Büntgen, U. and Tegel, W.: European tree-ring data and the Medieval Climate Anomaly, PAGES news, 19, 14–15, 2011.

Büntgen, U., Frank, D. C., Nievergelt, D., and Esper, J.: Summer temperature variations in the European Alps, AD 755–2004, Journal of Climate, 19, 5606–5623, 2006.

Büntgen, U., Trouet, V., Frank, D., Leuschner, H. H., Friedrichs, D., Luterbacher, J., and Esper, J.: Tree-ring indicators of German summer drought over the last millennium, Quaternary Science Reviews, 29, 1005–1016, 2010.

Büntgen, U., Brázdil, R., Heussner, K.-U., Hofmann, J., Kontic, R., Kyncl, T., Pfister, C., Chromá, K., and Tegel, W.: Combined dendro-documentary evidence of Central European hydroclimatic springtime extremes over the last millennium, Quaternary Science Reviews, 30, 3947–3959, 2011.

Fohlmeister, J., Schröder-Ritzrau, A., Scholz, D., Spöotl, C., Riechelmann, D. F., Mudelsee, M., Wackerbarth, A., Gerdes, A., Riechelmann, S., Immenhauser, A., et al.: Bunker Cave stalagmites: an archive for central European Holocene climate variability., Climate of the Past Discussions, 8, 2012.

Giguet-Covex, C., Arnaud, F., Poulenard, J., Disnar, J.-R., Delhon, C., Francus, P., David, F., Enters, D., Rey, P.-J., and Delannoy, J.-J.: Changes in erosion patterns during the Holocene in a currently treeless subalpine catchment inferred from lake sediment geochemistry (Lake Anterne, 2063 m asl, NW French Alps): the role of climate and human activities, The Holocene, 21, 651–665, 2011.

Gunnarson, B. E.: Temporal distribution pattern of subfossil pines in central Sweden: perspective on Holocene humidity fluctuations, The Holocene, 18, 569–577, 2008.

Haltia-Hovi, E., Saarinen, T., and Kukkonen, M.: A 2000-year record of solar forcing on varved lake sediment in eastern Finland, Quaternary Science Reviews, 26, 678–689, 2007.

Jong, R. d., Schoning, K., and Björck, S.: Increased aeolian activity during humidity shifts as recorded in a raised bog in south-west Sweden during the past 1700 years, Climate of the Past, 3, 411–422, 2007.

Kress, A., Hangartner, S., Bugmann, H., Büntgen, U., Frank, D. C., Leuenberger, M., Siegwolf, R. T., and Saurer, M.: Swiss tree rings reveal warm and wet summers during medieval times, Geophysical Research Letters, 41, 1732–1737, 2014.

Lamb, H. H.: The early medieval warm epoch and its sequel, Palaeogeography, Palaeoclimatology, Palaeoecology, 1, 13–37, 1965.

Linderholm, H. W. and Gunnarson, B. E.: Summer temperature variability in central Scandinavia during the last 3600 years, Geografiska Annaler: Series A, Physical Geography, 87, 231–241, 2005.

Ljungqvist, F. C., Krusic, P. J., Sundqvist, H. S., Zorita, E., Brattström, G., and Frank, D.: Northern Hemisphere hydroclimate variability over the past twelve centuries, Nature, 532, 94–98, 2016.

Magny, M., Arnaud, F., Billaud, Y., and Marguet, A.: Lake-level fluctuations at Lake Bourget (eastern France) around 4500–3500 cal. a BP and their palaeoclimatic and archaeological implications, Journal of Quaternary Science, 27, 494–502, 2012.

Mangini, A., Spötl, C., and Verdes, P.: Reconstruction of temperature in the Central Alps during the past 2000 yr from a $\delta 18O$ stalagmite record, Earth and Planetary Science Letters, 235, 741–751, 2005.

Martín-Chivelet, J., Muñoz-García, M. B., Edwards, R. L., Turrero, M. J., and Ortega, A. I.: Land surface temperature changes in Northern Iberia since 4000 yr BP, based on $\delta 13C$ of speleothems, Global and Planetary Change, 77, 1–12, 2011.

Mauquoy, D., Yeloff, D., Van Geel, B., Charman, D. J., and Blundell, A.: Two decadally resolved records from north-west European peat bogs show rapid climate changes associated with solar variability during the mid–late Holocene, Journal of Quaternary Science: Published for the Quaternary Research Association, 23, 745–763, 2008.

Ojala, A. E. and Alenius, T.: 10 000 years of interannual sedimentation recorded in the Lake Nautajärvi (Finland) clastic–organic varves, Palaeogeography, Palaeoclimatology, Palaeoecology, 219, 285–302, 2005.

Popa, I. and Kern, Z.: Long-term summer temperature reconstruction inferred from tree-ring records from the Eastern Carpathians, Climate dynamics, 32, 1107–1117, 2009.

Seim, A., Büntgen, U., Fonti, P., Haska, H., Herzig, F., Tegel, W., Trouet, V., and Treydte, K.: Climate sensitivity of a millennium-long pine chronology from Albania, Climate Research, 51, 217–228, 2012.

Sejrup, H., Lehman, S., Haflidason, H., Noone, D., Muscheler, R., Berstad, I., and Andrews, J.: Response of Norwegian Sea temperature to solar forcing since 1000 AD, Journal of Geophysical Research: Oceans, 115, 2010.

Sillasoo, U., Mauquoy, D., Blundell, A., Charman, D., Blaauw, M., Daniell, J. R., Toms, P., Newberry, J., Chambers, F. M., and Karofeld, E.: Peat multi-proxy data from Männikjärve bog as indicators of late Holocene climate changes in Estonia, Boreas, 36, 20–37, 2007.

Sümegi, P., Jakab, G., Majkut, P., Törőcsik, T., and Zatykó, C.: Middle Age paleoecological and paleoclimatological reconstruction in the Carpathian Basin, Ido;; járás QJ Hungarian Meteorol. Service, 113, 265–298, 2009.

Swierczynski, T., Brauer, A., Lauterbach, S., Martín-Puertas, C., Dulski, P., von Grafenstein, U., and Rohr, C.: A 1600 yr seasonally resolved record of decadal-scale flood variability from the Austrian Pre-Alps, Geology, 40, 1047–1050, 2012.

Taricco, C., Ghil, M., Alessio, S., and Vivaldo, G.: Two millennia of climate variability in the Central Mediterranean, Climate of the Past, 5, 171–181, 2009.

Tiljander, M., Karhu, J. A., and Kauppila, T.: Holocene records of carbon and hydrogen isotope ratios of organic matter in annually laminated sediments of Lake Korttajärvi, central Finland, Journal of Paleolimnology, 36, 233–243, 2006.

Väliranta, M., Korhola, A., Seppä, H., Tuittila, E.-S., Sarmaja-Korjonen, K., Laine, J., and Alm, J.: High-resolution reconstruction of wetness dynamics in a southern boreal raised bog, Finland, during the late Holocene: a quantitative approach, The Holocene, 17, 1093–1107, 2007.

Van Engelen, A. F., Buisman, J., and IJnsen, F.: A millennium of weather, winds and water in the Low Countries, in: History and climate, pp. 101–124, Springer, 2001.

Vasskog, K., Paasche, Ø., Nesje, A., Boyle, J. F., and Birks, H.: A new approach for reconstructing glacier variability based on lake sediments recording input from more than one glacier, Quaternary Research, 77, 192–204, 2012.

Wilhelm, B., Arnaud, F., Sabatier, P., Crouzet, C., Brisset, E., Chaumillon, E., Disnar, J.-R., Guiter, F., Malet, E., Reyss, J.-L., et al.: 1400 years of extreme precipitation patterns over the Mediterranean French Alps and possible forcing mechanisms, Quaternary Research, 78, 1–12, 2012.

Zanchetta, G., Van Welden, A., Baneschi, I., Drysdale, R., Sadori, L., Roberts, N., Giardini, M., Beck, C., Pascucci, V., and Sulpizio, R.: Multiproxy record for the last 4500 years from Lake Shkodra (Albania/Montenegro), Journal of Quaternary Science, 27, 780–789, 2012.